AIAA JOURNAL
Vol. 39, No. 10, October 2001

Structurally Nonlinear Fluttering Airfoil in Turbulent Flow

Dominique C. Poirel*
Royal Military College of Canada, Kingston, Ontario K7K 7B4, Canada
and
Stuart J. Price†
McGill University, Montreal, Quebec H3A 2K6, Canada

The dynamics and response of a structurally nonlinear two-dimensional airfoil in turbulent flow are investigated numerically. The solution is analyzed in terms of probability density function (PDF), response mean square, power spectral density, and Lyapunov exponent. Both the longitudinal and vertical components of turbulence are considered. It is shown that turbulent flow, due to its longitudinal component, diminishes the stability of the aeroelastic system by advancing the flutter point and decreasing the damping, thus confirming results from previous work where only the longitudinal component was modeled. Furthermore, the shift in flutter airspeed is strongly dependent on the random stiffness terms. It is also observed that turbulence may advance the airspeed at which the pitch angle marginal PDF changes from uni- to bimodal compared with the nonexcited deterministic case, whereas the heave transition appears to be postponed. This observation is attributed to the nonlinearity considered, a cubic stiffness in torsion. Finally, in terms of response mean square, the system appears to be more sensitive to the presence of the longitudinal excitation component at pre- rather than at postinstability airspeeds.

Nomenclature

$A_1, A_2,$ b_1, b_2	=	coefficients in Wagner's function two-lag-terms representation
$A_3, A_4,$ b_3, b_4	=	coefficients in Kussner's function two-lag-terms representation
a_h	=	nondimensional distance between elastic axis and midchord
b	=	semichord
G_{wn}	=	Gaussian white noise
h, θ	=	airfoil motion in heave and pitch directions
I_{cg}	=	airfoil moment of inertia about center of mass
K_h, K_θ	=	linear heave and pitch stiffness
K_3	=	cubic pitch stiffness
k	=	reduced frequency, $\omega b/U_m$
k_3	=	nondimensional cubic pitch stiffness, K_3/K_θ
L_{nd}	=	nondimensional scale of turbulence, L/b
$L(t), M_{\text{ea}}$	=	lift force and aerodynamic moment about the elastic axis
$L_\Phi, M_{\text{ea}\Phi}$	=	lift force and aerodynamic moment due to arbitrary motion and longitudinal turbulence
$L_\Psi, M_{\text{ea}\Psi}$	=	lift force and aerodynamic moment due to vertical turbulence
m	=	airfoil mass per unit length
r_θ	=	nondimensional radius of gyration, I_{ea}/mb^2
t	=	time
U	=	total freestream velocity, $U_m + u_T$
U_m	=	mean freestream velocity
$U_{m,\text{nd}}$	=	nondimensional mean freestream velocity
U_{nd}	=	nondimensional speed, $U/b\omega_\theta$
$\bar{u}, \bar{w}$	=	normalized (by the mean freestream) freestream and vertical turbulence velocities
u_T, w_T	=	turbulence velocities
$u_{T,\text{nd}}, w_{T,\text{nd}}$	=	nondimensional turbulence velocities
$w_{3/4}$	=	downwash at three-quarter chord
x_θ	=	nondimensional distance between elastic axis and center of mass
z_1, z_1'	=	nondimensional aerodynamic lag states due to Wagner's function
z_2, z_2'	=	nondimensional aerodynamic lag states due to Kussner's function
α	=	angle of attack
$\lambda_{\text{max,nd}}$	=	nondimensional largest Lyapunov exponent, $\lambda_{\max} b/\sigma_T$
μ	=	nondimensional airfoil mass, $m/\rho\pi b^2$
ρ	=	density of air
σ_T^2	=	turbulence velocity variance
$\sigma_{T,\text{nd}}^2$	=	nondimensional turbulence velocity variance, $\sigma_T^2/(b\omega_\theta)^2$
τ	=	nondimensional time, $U_m t/b$
$\Phi(t)$	=	Wagner's function
$\phi_{\text{lT}}, \phi_{\text{vT}}$	=	longitudinal and vertical turbulence power spectral densities
ϕ_{wn}	=	white noise power spectral density
$\Psi(t)$	=	Kussner's function
ω	=	radial frequency
ω_h, ω_θ	=	radial frequencies in heave and pitch
$\dot{}$	=	derivative with respect to dimensional time
$'$	=	derivative with respect to nondimensional time, $\mathrm{d}/\mathrm{d}\tau$

Received 3 August 1999; revision received 5 October 2000; accepted for publication 13 April 2001.

*Assistant Professor, Department of Mechanical Engineering. Senior Member AIAA.
†Professor, Department of Mechanical Engineering. Senior Member AIAA.

Introduction

THE dynamics and response of a structurally nonlinear two-dimensional airfoil in turbulent flow are investigated numerically. Both the longitudinal and vertical components of turbulence are considered. This work is a continuation of Ref. 1, where only the longitudinal component of turbulence was considered.

The motivation for this work is both the ubiquitous nature of turbulence coupled with the ever increasing practical importance of nonlinearities, as well as the theoretical challenge and intellectual significance that the combined problem of random excitations and nonlinearities offers.

The general random nonlinear problem has been studied for some time, for example, by Stratonovich[2] in physics and Ibrahim[3] in engineering. Recently, however, there has been a renewal in the approach taken in light of new developments in chaos and related nonlinear

dynamics, namely, from a bifurcation analysis point of view. This aspect has clearly been identified in the physical and mathematical sciences and is starting to obtain full recognition in engineering related fields. At the risk of missing a number of important contributors, one can think, for example, of the work of Arnold et al.,[4] in mathematics, Horsthemke and Lefever[5] or Knobloch and Weisenfeld[6] in physics–chemistry, and Ariaratnam[7] in engineering.

With regards specifically to the aeroelastic problem, random excitation usually takes the form of turbulence, or more specifically turbulent flow, which can originate from a number of different sources. These sources range in intensity from acoustic emission, geothermal (atmospheric) conditions to the high intensity excitation of separated flow in the wake of an object, as well as vortex breakdown leading to what is known as tail buffet.[8]

Application to the aeroelastic problem is, thus, evident, but relatively little work on the nonlinear case has been published so far. In this regard, most of the literature is concerned with random nonlinear panel flutter. See, for example, the work of Ibrahim et al.[9] for the in-plane loading or Abdel-Motagaly et al.[10] for the vertical excitation. Another recent work, by Romberg and Popp,[11] deals with the influence of turbulence on a flexible tube. Le Maître et al.[12] have given a more exotic flavor to the problem by investigating the interaction of atmospheric turbulence and a sail. Also noteworthy is the work of Lin[13] on random wind-excited bridges and Prussing and Lin[14] on rotor blades in atmospheric turbulence and turbulent wake. However, these last authors limited their analysis to linear problems.

A secondary issue is the influence of the longitudinal component of the excitation. As exemplified by various design standards,[15,16] modeling of the longitudinal component of turbulence (atmospheric in this case) is commonly neglected in aircraft aeroelastic analyses. This approach can be considered as part of the so-called accepted engineering practice. However, we are unaware of any formal justification, theoretical or experimental, to that effect within the published literature or of any reference to it in relatively recent papers. The closest to any type of rationale that has been found supporting this approximation is offered by Hoblit,[17] who makes a very rudimentary comparison of the lift force, with and with out longitudinal excitation, on a rigid aircraft. Even in the very comprehensive exposé on the dynamic response of aircraft to atmospheric turbulence by Houbolt et al.,[18] the impact of the longitudinal component is discarded rather freely.

It is presumed that there are two basic reasons for "neglecting" longitudinal turbulence in aeroelastic analyses. First, it is a common belief that for many applications the relative contribution of the longitudinal excitation is much lower than the vertical (and lateral for a three-dimensional model) component; hence, it can be treated as a secondary effect via a correction factor to the vertical excitation. Second, the mathematical treatment of the aeroelastic problem is complicated considerably by the introduction of the longitudinal excitation. The main complication is that the longitudinal excitation transforms the externally forced time-invariant system into a parametrically excited, hence, time-varying, problem. In view of the preceding comments, particular attention will be paid to the influence of the longitudinal component of turbulence on the nonlinear airfoil.

The main objective of this paper is to investigate the effect of turbulent flow on a two-dimensional flexible airfoil when a structural nonlinearity is considered. In pursuit of this primary goal, a subobjective is an attempt to articulate a more detailed and comprehensive picture of the relative contribution of the longitudinal component of turbulence, in the presence of the vertical excitation, as experienced by an airfoil.

Problem Description

Turbulence Modeling

In this work, turbulence is modeled as a random process. The stochastic treatment of turbulence usually requires a number of simplifications. Some of the simplifications used here are Taylor's (and von Kármán's) hypothesis, or the frozen turbulence assumption; a Gaussian distribution; chordwise (only used for the longitudinal component as discussed later) and vertical uniformity; and isotropy and statistical stationarity.[18,19] These simplifications permit the two turbulence components to be expressed as functions of time only, $w_T = w_T(t)$ and $u_T = u_T(t)$, and the airspeed is then given by

$$U(t) = U_m + u_T(t) \tag{1}$$

It is common to represent an isotropic turbulent field by its double velocity correlation matrix, where, due to isotropy, only the diagonal terms are nonzero.[20] These diagonal terms represent the longitudinal and vertical components of the two-dimensional turbulence. From these correlation functions power spectra can be developed because these two entities form Fourier transform pairs. Assuming that the spectral content of turbulence is provided by the Dryden model, the one-sided power spectral density (PSD) longitudinal representation in terms of the temporal radian frequency is given as[17–19]

$$\phi_{\mathrm{lT}}(\omega) = \sigma_T^2 (2L/\pi U_m)\left\{1 \Big/ \left[1 + (L\omega/U_m)^2\right]\right\} \tag{2a}$$

and the vertical component is

$$\phi_{\mathrm{vT}}(\omega) = \sigma_T^2 \left(\frac{L}{\pi U_m}\right) \frac{1 + 3[L\omega/U_m]^2}{\left[1 + (L\omega/U_m)^2\right]^2} \tag{2b}$$

They are presented in nondimensional form in Fig. 1 for a scale of turbulence and variance, $L_{\mathrm{nd}} = 50.0$ and $\sigma^2_{T,\mathrm{nd}} = 1.0$, respectively. In comparison with the turbulence spectrum, note that the flutter frequency coalescence for the particular example used here occurs at approximately $k = 0.18$.

It can be shown that the scale of turbulence L divided by the mean freestream velocity U_m is equal to the correlation time of the longitudinal random excitation, whereas the correlation time of the vertical random excitation is half of that ratio, that is, $L/(2U_m)$. In the context of this paper, a physical interpretation of the scale of turbulence is the "average" distance traveled by the airfoil during which the turbulence velocities can be considered as uniform. Hence, the larger the scale of turbulence, the farther, in average, the airfoil may travel before experiencing a

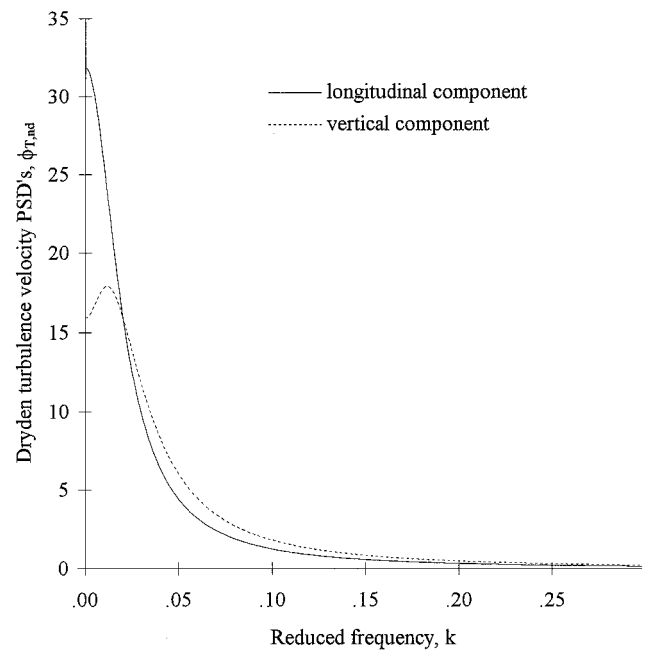

Fig. 1 Nondimensional PSD of the Dryden turbulence model for $L_{\mathrm{nd}} = 50.0$ and $\sigma^2_{T,\mathrm{nd}} = 1.0$; closed-form solution.

change in turbulence velocities. Thus, it may be assumed that for large magnitudes of scale of turbulence the velocity over the airfoil is nearly uniform at any instant in time, hence chordwise uniformity.

The frequency-domain Dryden turbulence model can be transformed into the time domain in the form of stochastic differential equations (SDEs), with the vertical and longitudinal turbulence velocities acting as dependant variables and Gaussian white noise as an external forcing with $\phi_{\text{wn}} = 1$. The procedure consists of developing a transfer function in the Laplace domain that relates Gaussian white noise as input and turbulence velocity as output. The square of the modulus of the transfer function, expressed in the frequency domain, must match the turbulence PSD given in Eqs. (2). Taking the inverse Laplace transform of the transfer functions gives the time-domain representation, as shown in the following:

$$\dot{u}_T(t) + u_T(t)(U_m/L) = \sigma_T(2U_m/\pi L\phi_{\text{wn}})^{\frac{1}{2}} G_{\text{wn}}(t)$$

$$\ddot{w}_T(t) + \dot{w}_T(t)(2U_m/L) + w_T(t)\left(U_m^2/L^2\right)$$

$$= \sigma_T\left(U_m^3/\pi L^2\phi_{\text{wn}}\right)^{\frac{1}{2}} G_{\text{wn}}(t) + \sigma_T(3U_m/\pi L\phi_{\text{wn}})^{\frac{1}{2}} \dot{G}_{\text{wn}}(t) \quad (3)$$

Equations (3) are then used as inputs to the aeroelastic equations of motion (8), via the aerodynamic loads, Eqs. (5) and (7).

Airfoil Structural Modeling

The airfoil is modeled as a rigid flat plate, with degrees of freedom in pitch and heave; structural flexibility is provided by torsional and translational springs. A cubic representation of the torsional spring is considered; this is the only source of nonlinearity. Other nonlinearities, such as the geometric terms have been neglected; thus, oscillations are limited to small amplitudes. Structural damping is also neglected. Damping is provided by the aerodynamics as described in the next section. The structural equations, obtained from Fung,[19] are modified to include the nonlinearity. The heave is defined as positive downward and the pitch nose up,

$$m\ddot{h} + mx_\theta b\ddot{\theta} + K_h h = -L(t)$$

$$\left[I_{\text{cg}} + mx_\theta^2 b^2\right]\ddot{\theta} + mx_\theta b\ddot{h} + K_\theta\theta + K_3\theta^3 = M_{\text{ea}}(t) \quad (4)$$

The lift force $L(t)$ and aerodynamic moment $M_{\text{ea}}(t)$ acting on the right-hand side of Eqs. (4) are described in the next section.

Aerodynamic Modeling

Only attached flow with small amplitude oscillations are considered; hence, the aerodynamics is linear. The unsteady aerodynamics, accounting for memory effects, is modeled, assuming incompressible inviscid flow, via Duhamel's integral and the two-state representation of Wagner's function given by Jones (see Ref. 19). This aerodynamic model is extended to include a random time-varying airspeed based on the work of van der Wall and Leishman.[21] The airspeed is assumed to be uniformly distributed chordwise. Other details are provided in Ref. 1. Aerodynamic forces due to random variations of the freestream velocity, and accounting for arbitrary pitch and heave motions, are modeled by the following (the pitch angle and angle of attack are taken to be equal):

$$L_\Phi(t) = \pi\rho b^2[\ddot{h} + U\dot{\alpha} - ba_h\ddot{\alpha}]$$

$$+ 2\pi\rho bU\left[w_{\frac{3}{4}}\Phi(0) - \int_0^t w_{\frac{3}{4}}(s)\frac{\mathrm{d}\Phi(t-s)}{\mathrm{d}s}\,\mathrm{d}s\right]$$

$$M_{\text{ea}\Phi}(t) = \pi\rho b^2\left\{ba_h\ddot{h} - b[0.5 - a_h]U\dot{\alpha} - b^2\left[a_h^2 + \tfrac{1}{8}\right]\ddot{\alpha}\right\}$$

$$+ 2\pi\rho b^2[a_h + 0.5]U\left[w_{\frac{3}{4}}\Phi(0) - \int_0^t w_{\frac{3}{4}}(s)\frac{\mathrm{d}\Phi(t-s)}{\mathrm{d}s}\,\mathrm{d}s\right] \quad (5)$$

where

$$w_{\frac{3}{4}}(t) = \dot{h} + U\alpha + b[0.5 - a_h]\dot{\alpha}$$

$$\Phi(t) = 1 - 0.165\exp(-0.0455U_m t/b) - 0.335\exp(-0.3U_m t/b)$$

Aerodynamic forces and moment are also generated by the presence of vertical turbulence, which in effect changes the local angle of attack on the airfoil. Because of the finite time associated with penetration of a discrete gust around the airfoil, the aerodynamics exhibit a gradual increase in magnitude. These unsteady effects are expressed in terms of $\Psi(t)$, Kussner's function. Note that the simplification of chordwise uniformity is neither required nor used for the vertical turbulence, as demonstrated in the following. The gust-penetration function $\Psi(t)$ represents the growth of circulation as a sharp-edged gust strikes the leading edge of the airfoil in incompressible flow. Similarly to Wagner's function, it can be expressed by a two-state representation[22]:

$$\Psi(t) = 1 - 0.5792\exp(-0.1393U_m t/b) - 0.4208$$

$$\times \exp(-1.802U_m t/b) \quad (6)$$

Using Duhamel's superposition integral, the force and moment due to vertical turbulence can be derived in the same manner as that used for the lift and aerodynamic moment due to arbitrary motion and freestream variations. Differences between the two set of expressions are the downwash at the three-quarter chord, which is replaced by the vertical gust (equivalent to the downwash at the leading edge), and the absence of apparent mass terms, that is, no air mass is displaced by the airfoil motion in this case. In effect, Duhamel's superposition integral enables the use of Kussner's function, originally derived for a discrete gust, to be employed in the problem of continuous turbulence. The expressions are

$$L_\Psi(t) = 2\pi\rho bU\left[w_T\Psi(0) - \int_0^t w_T(s)\frac{\mathrm{d}\Psi(t-s)}{\mathrm{d}s}\,\mathrm{d}s\right]$$

$$M_{\text{ea}\Psi}(t) = 2\pi\rho b^2[a_h + 0.5]U\left[w_T\Psi(0) - \int_0^t w_T(s)\frac{\mathrm{d}\Psi(t-s)}{\mathrm{d}s}\,\mathrm{d}s\right] \quad (7)$$

The aeroelastic equations of motion are formed by combining Eqs. (4), (5), and (7) and by introducing the equivalency between angle of attack and angle of pitch because no angle of incidence is considered. The integro-differential form of these equations is transformed into differential form by introducing four additional states. These four states originate from the two lag terms in Wagner's function and two lag terms in Kussner's function. Some details are provided in Ref. 1. The transformation of the aeroelastic equations into pure differential form enables a physical interpretation of the different terms from the point of view of the traditional mechanical system model with inertia, damping, and stiffness forces and an external forcing; it also facilitates the numerical integration procedure. The nondimensional aeroelastic equations of motion are given in differential form:

$$
\begin{bmatrix}
1+\dfrac{a_h^2+\frac{1}{8}}{\mu r_\theta^2} & \dfrac{x_\theta}{r_\theta^2}-\dfrac{a_h}{\mu r_\theta^2} & 0 & 0\\
x_\theta-\dfrac{a_h}{\mu} & 1+\dfrac{1}{\mu} & 0 & 0\\
0 & 0 & 1 & 0\\
0 & 0 & 0 & 1
\end{bmatrix}
\begin{Bmatrix}\theta''\\ \xi''\\ z_1''\\ z_2''\end{Bmatrix}
$$

$$
+\begin{bmatrix}
\dfrac{\bar{u}(0.5-a_h)}{\mu r_\theta^2} & -\dfrac{(a_h+0.5)(0.5-a_h)\bar{u}}{\mu r_\theta^2} & -\dfrac{(a_h+0.5)\bar{u}}{\mu r_\theta^2} & -\dfrac{2(a_h+0.5)(A_1b_1+A_2b_2)\bar{u}}{\mu r_\theta^2} & -\dfrac{2(a_h+0.5)(A_3b_3+A_4b_4)}{\mu r_\theta^2}\\
\dfrac{\bar{u}}{\mu} & +\dfrac{(0.5-a_h)\bar{u}}{\mu} & \dfrac{\bar{u}}{\mu} & \dfrac{2(A_1b_1+A_2b_2)\bar{u}}{\mu} & \dfrac{2(A_3b_3+A_4b_4)}{\mu}\\
-(0.5-a_h) & & -1 & b_1+b_2 & 0\\
0 & & 0 & 0 & b_3+b_4
\end{bmatrix}
\begin{Bmatrix}\theta'\\ \xi'\\ z_1'\\ z_2'\end{Bmatrix}
$$

$$
+\begin{bmatrix}
\dfrac{1}{U_{m,\mathrm{nd}}^2}-\dfrac{(a_h+0.5)\bar{u}^2}{\mu r_\theta^2} & 0 & -\dfrac{(a_h+0.5)b_1b_2\bar{u}^2}{\mu r_\theta^2} & -\dfrac{2(a_h+0.5)b_3b_4}{\mu r_\theta^2}\\
\dfrac{\bar{u}^2}{\mu} & \dfrac{\bar{\omega}^2}{U_{m,\mathrm{nd}}^2} & \dfrac{b_1b_2\bar{u}}{\mu} & \dfrac{2b_3b_4}{\mu}\\
-\bar{u} & 0 & b_1b_2 & 0\\
0 & 0 & 0 & b_3b_4
\end{bmatrix}
\begin{Bmatrix}\theta\\ \xi\\ z_1\\ z_2\end{Bmatrix}
+\begin{bmatrix}
\dfrac{k_3}{U_{m,\mathrm{nd}}^2} & 0 & 0 & 0\\
0 & 0 & 0 & 0\\
0 & 0 & 0 & 0\\
0 & 0 & 0 & 0
\end{bmatrix}
\begin{Bmatrix}\theta^3\\ \xi^3\\ z_1^3\\ z_2^3\end{Bmatrix}
=\begin{Bmatrix}0\\0\\0\\ \bar{w}\end{Bmatrix}
\tag{8}
$$

where

$$\bar{u}=U(t)/U_m=U_{\mathrm{nd}}(\tau)/U_{m,\mathrm{nd}}=1+u_{T,\mathrm{nd}}(\tau)/U_{m,\mathrm{nd}}$$

$$\bar{w}=w_T(t)/U_m=w_{T,\mathrm{nd}}(\tau)/U_{m,\mathrm{nd}}$$

and $A_1=0.165$, $A_2=0.335$, $A_3=0.5792$, $A_4=0.4208$, $b_1=0.0455$, $b_2=0.3$, $b_3=0.1393$, and $b_4=1.802$.

A few remarks on these random nonlinear differential equations are in order. First, both the damping and stiffness matrices are timevarying or parametrically excited. This is due to the longitudinal turbulence excitation, which enters the problem by means of the aerodynamic loads. Longitudinal turbulence acts as a linear colored random excitation on the damping terms via velocity $\bar{u}$. The excitation on the stiffness terms is both linear and quadratic, via $\bar{u}$ and $\bar{u}^2$, respectively. On the other hand, the mass matrix is time invariant. The nonlinear stiffness matrix is also time invariant because it represents the nonlinear torsional structural spring. Had nonlinear aerodynamics been modeled, the random excitation would also have acted on the nonlinear forces. Furthermore, the vertical component of turbulence acts as an external forcing.

Specifically with regard to the random terms in the damping matrix, it is not expected that they have a significant impact on the stability of the excited airfoil because, for the deterministic problem, the physical mechanism of the flutter instability is essentially dictated by the aeroelastic stiffness and inertia properties. More precisely, the type of flutter investigated is the classical, or binary, flutter, which is characterized by the frequency coalescence of two aeroelastic modes.[19] It is this coalescence that enables the transfer of energy from the airflow to the airfoil required for the flutter instability. Accordingly, the stiffness and inertia terms, shown as inertia and stiffness matrices in Eqs. (8), are mainly responsible for the classical flutter instability, whereas the damping matrix plays a minor role. Thus, we anticipate to observe the same relative importance of random stiffness terms over random damping terms for random (or stochastic) flutter.

Numerical Simulation

The eighth-order aeroelastic system [Eqs. (8)] along with the nondimensional form of the turbulence SDEs [Eqs. (3)] are then expressed in state-space form and solved numerically using a fourth-order Runge–Kutta algorithm. Based on the Box–Muller algorithm and with the help of an uniform random number generator, RAN1,[23] Gaussian white noise is generated at each time step of the integration and fed into the aeroelastic-turbulence system. Different uniform random numbers are used for the vertical and longitudinal differential equations. This is justified physically by the hypothesis of isotropy of the turbulent field, which leads to a diagonal double velocity correlation matrix, hence, uncorrelated velocity components. Furthermore, from a more practical perspective, it was noted that using the same random numbers for both components lead to a skewed probability density function (PDF) in heave, which is not reasonable due to the symmetry of the problem. Note that a random number generator proposed in the first edition of Ref. 23 appeared to introduce artificial peaks in the response frequency spectrum and, thus, was not used.

The time step in the integration is chosen in accordance with both the scale of turbulence, or noise correlation time, and with the aeroelastic modal frequencies. The integration is performed until steady state is obtained in both the statistical properties and the PDF of the system response. For the cases considered in this paper, the limiting criterion for the time step is the noise correlation time; hence, the time step is chosen to be at most $\frac{1}{25}$th of the nondimensional scale of turbulence. On average, iterations were performed for 50×10^6 time steps, whereas steady state was obtained after 1×10^6 steps. The process is also assumed to be ergodic, thus, providing an equivalency between ensemble and time averages. In this regard, all of the dynamic information is contained in one sample response. Further details on the numerical modeling may be found in Ref. 1.

The cases presented are for an airfoil with the following nondimensional airfoil parameters: $k_3=400$, $\omega_h/\omega_\theta=0.6325$, $x_\theta=0.25$, $r_\theta=0.5$, $\mu=100$, and $a_h=-0.5$. As introduced earlier, the problem is investigated in the context of one of the most common aeroelastic instability types, namely, classical flutter. For the set of parameters chosen, the deterministic flutter speed is $U_{f,\mathrm{nd}}=4.31$. At lower airspeeds, the equilibrium point is stable. For airspeeds above the flutter speed, the equilibrium point is unstable. However, due the presence of the cubic nonlinear hardening torsional spring, the postflutter dynamics is attracted toward a stable limit-cycle oscillation. Accordingly, for the deterministic problem, the flutter point corresponds to a supercritical Hopf bifurcation.

Note that most results shown are for a scale of turbulence $L_{\mathrm{nd}}=50.0$ and a turbulence variance $\sigma_{T,\mathrm{nd}}^2=1.0$. When the deterministic flutter speed is used as the reference velocity, the turbulence intensity is 23%. Although this is a relatively high level of intensity, it is chosen to exemplify better and to gain some insight into the qualitative impact of the presence of turbulence. Lower intensities

(not shown here) have also been investigated and exhibit similar behavior. For example, see Ref. 1 for the longitudinal case. Note, as well, that Romberg and Popp[11] have experimentally generated turbulence intensity levels between 10 and 23%, with a grid, for their investigation of a flexible tube. To put the turbulence intensity in perspective, atmospheric turbulence intensity levels would range from 1 to 5% based on a flutter speed of 500 kn and on rms values of turbulence velocities given by Houbolt et al.[18] Turbulence intensity levels in the order of 14% could be obtained if velocity fluctuations due to separated flow in the wake of object (for example, a rotor blade according to Fujimori et al.[24]), superimposed on atmospheric excitation, are considered. On the higher end of the scale, leading-edge vortex breakdown[8,25] can induce turbulence intensity levels in the order of 30%, perhaps more.

The main measures used to describe the dynamic behaviour are the pitch and heave response marginal PDFs and the mean square responses. The PDF is useful particularly for stochastic bifurcations. Power spectra, Lyapunov exponents, and time histories (not shown here) have also been generated to complement the analysis.

PDF Analysis

The flutter problem for a structurally nonlinear airfoil excited by pure longitudinal turbulence has been investigated previously, and results are presented in Ref. 1. In brief, and in comparison with the nonexcited, deterministic system, the main observations and conclusions were an advancement of the flutter airspeed, postponement of the supercritical Hopf bifurcation leading to a stochastic limit-cycle oscillation (LCO) characterized by a transition from a uni- to a bimodal PDF, and the appearance of a third dynamic region, between these two airspeeds, characterized by a sharp single-peaked PDF centered about the equilibrium point. For the turbulence values given earlier, the advanced flutter speed occurred at $U_{m,\mathrm{nd}} = 3.65$ compared with 4.31 for zero turbulence and was associated with the concept of dynamical (D)-bifurcation. The postponed LCO onset occurred at $U_{m,\mathrm{nd}} = 4.71$ and was associated with a phenomenological (P)-bifurcation. Loosely speaking, a D-bifurcation corresponds to a loss of stability as expressed by a change of sign of the largest Lyapunov exponent and, hence, is associated with a critical slow down of the dynamics in the same manner as the deterministic dynamics is. On the other hand, the P-bifurcation defines a qualitative change in the dynamic behavior as represented by the PDF. For a detailed and rigorous treatment of the subject, see Refs. 4–7.

When the same system is excited with both longitudinal and vertical components of turbulence, only two regions of different dynamic behavior are observed (Fig. 2). They are characterized by a Gaussian-like PDF at low airspeeds, followed by a transition into a bimodal probability density for the pitch, but staying unimodal for the heave even at relatively high airspeeds ($U_{m,\mathrm{nd}} \approx 25$), well past the flutter region. In addition, for the cases investigated, the range

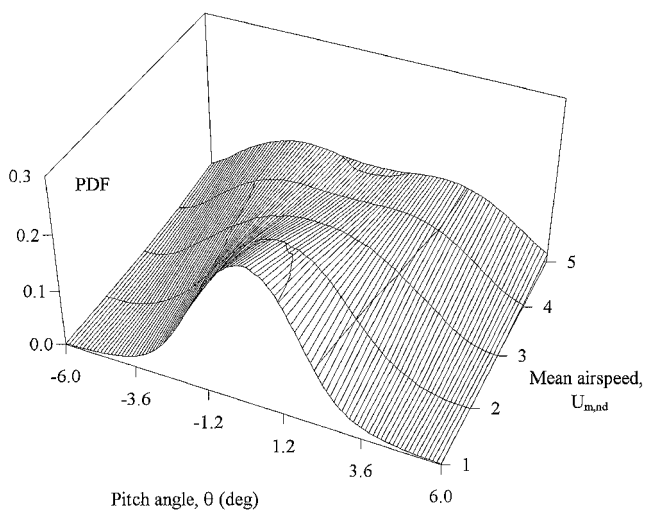

Fig. 2 Bifurcation diagram of the airfoil PDF pitch response for the combined excitation case; $L_{\mathrm{nd}} = 50.0$ and $\sigma^2_{T,\mathrm{nd}} = 1.0$.

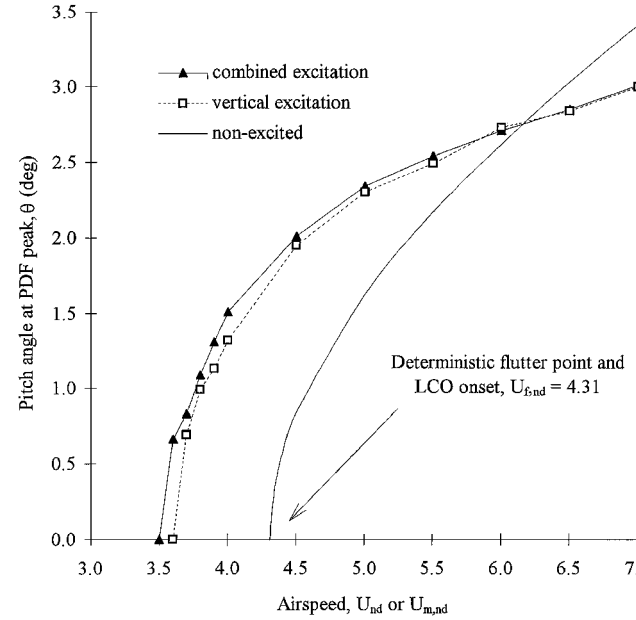

Fig. 3 Bifurcation diagram of the airfoil pitch response for the combined excitation, vertical excitation, and nonexcited cases; $L_{\mathrm{nd}} = 50.0$ and $\sigma^2_{T,\mathrm{nd}} = 1.0$.

of airspeeds within which the transition in pitch PDF occurs is, in general, lower than either the deterministic or the stochastic flutter points defined in Ref. 1, where only longitudinal excitation was considered (Fig. 3). If the longitudinal component is not considered, leaving only the vertical excitation, the same type of PDFs obtained with the combined excitation are observed; however, one difference is that the pitch transition from unimodal to bimodal behavior occurs at higher airspeeds, but still generally lower than the flutter speeds obtained in Ref. 1 (Fig. 3). Here also, the heave response stays unimodal.

The variation with airspeed of the magnitude of the pitch angle at the PDF peaks, which is the stochastic equivalent of the deterministic LCO amplitude, has an interesting behavior. Because of the advanced transition from a uni- to bimodal probability density due to the longitudinal excitation, the pitch PDF peaks of the vertically excited system are initially closer to each other than for the combined excitation case. However, past a certain airspeed no distinction in the peak location can be made between the two cases. In other words, the rate at which the peak splitting happens is smaller for the combined excitation case. A second observation, also shown in Fig. 3, indicates that the stochastic LCO pitch amplitude, which is initially higher than the nonexcited LCO, becomes smaller than its deterministic counterpart. Eventually, the stochastic LCO pitch amplitude will tend to the nonexcited amplitude but at a much higher airspeed.

The observations presented, based on the pitch and heave probability densities, lead to the following interpretations. From purely a physical point of view, it may be tempting to conclude that the pitch uni- to bimodal transition is in fact a bifurcation of the stochastic equilibrium point and that the heave has not bifurcated. However, the identification of a bifurcation must refer to the response of the aeroelastic system as a whole. In our case, the system is multidimensional, thus, strictly speaking, requires a multidimensional, or joint, PDF for a complete description. We may also be tempted to use the argument that because, for a linear system, the instability point does not depend on any external forcing, deterministic or stochastic, the observed advanced transition in pitch due to vertical turbulence is purely an artifice of the marginal PDF and is not a bifurcation. However, for nonlinear systems, the situation is not that clear. Although we know that for deterministic nonlinear systems the bifurcation landscape depends on the external forcing, the picture becomes blurred if the forcing is stochastic. Except for the single variable system excited by additive Gaussian white noise for which it has been shown theoretically that the bifurcation is not

influenced by the noise, at least when simple local bifurcation types such as Hopf or pitchfork are considered,[5,26] published literature on multidimensional and/or colored noise excited systems is contradictory. For example, Knobloch and Weisenfeld[6] discuss the case of a single degree of freedom (DOF), that is, two-dimensional, system excited by additive Gaussian white noise, which has no effect on the bifurcation point. Lugiato et al.[27] and Schimansky-Geier et al.[28] show examples of the contrary.

On the other hand, considering the presence of the longitudinal component of turbulence, it is believed that the pitch PDF incremental advanced transition from uni- to bimodal behavior truly represents a change in bifurcation airspeed. However, the actual magnitude of the shift in bifurcation airspeed cannot be precisely determined with the current analysis tools available.

On a more practical note, there is a possible physical explanation for the early uni- to bimodal transition of the pitch response as opposed to the heave, which is as follows. The cubic nonlinearity is felt directly by the pitch DOF, but only indirectly by the heave through coupling terms. In other words, the Gaussian-like probability density of the heave response is preserved for a longer range of airspeed. Perhaps this behavior is slightly accentuated by the fact that for this analysis the elastic axis is located exactly at the aerodynamic center, that is, $a_h = -0.5$; thus, the pitch DOF is not directly excited by the vertical turbulence, but only indirectly through coupling terms.

Mean Square Analysis

In terms of either the mean square pitch or heave response, the response intensity for the combined excitation is, not surprisingly, larger than for the vertical excitation case for all airspeeds investigated. The response curves show some interesting characteristics, particularly at the two extremes of the airspeed range. At higher airspeeds, the mean square of the pitch response for both the vertical and combined excitation cases behave linearly with airspeed and increase at the same rate (Fig. 4). Consequently, for this high-airspeed range, the absolute contribution of the longitudinal component on the total pitch response remains constant, but its relative impact diminishes as the total response increases.

When analyzing the mean square heave response, it is remarkable that, similarly to the pitch, the absolute contribution of the longitudinal component remains constant for increasing airspeed, but contrary to pitch, the responses do not settle on a linear trend (Fig. 5). This difference in behavior is attributed also to the location of the nonlinearity, which directly affects the pitch response but only indirectly affects the heave. In this regard, note from Figs. 4 and 5 that, contrary to the heave, the pitch bifurcation landscape for the deterministic nonexcited problem remains close to the simplest expression of the Hopf normal form. This is characterized by

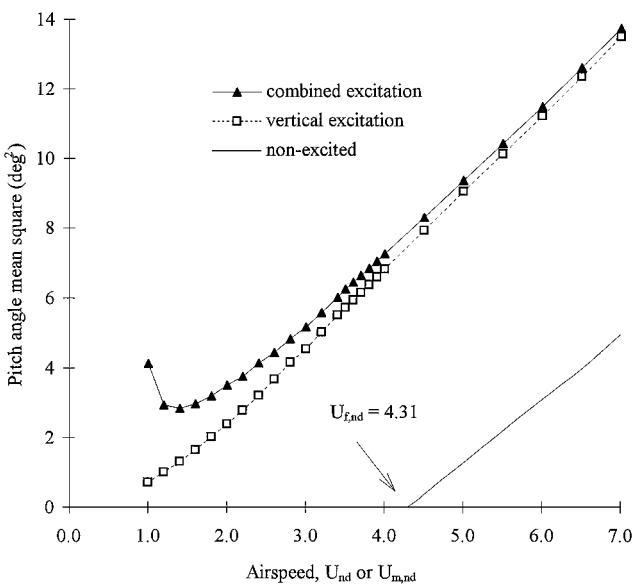

Fig. 4 Airfoil pitch mean square response for the combined excitation, vertical excitation, and nonexcited cases; $L_{nd} = 50.0$ and $\sigma^2_{T,nd} = 1.0$.

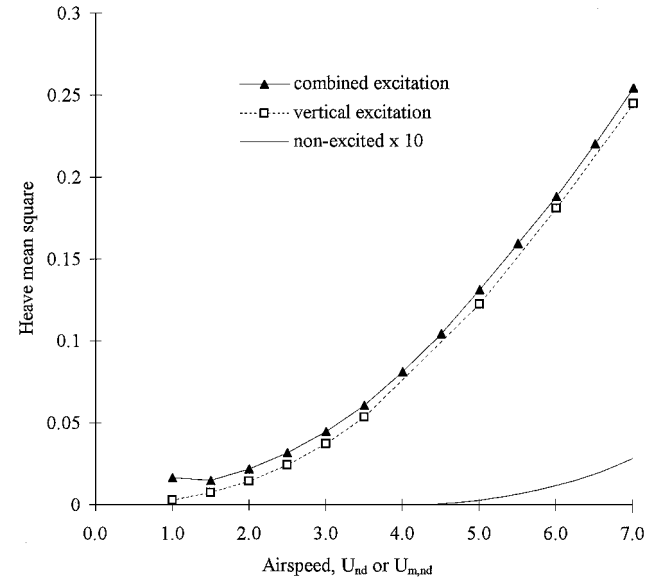

Fig. 5 Airfoil heave mean square response for the combined excitation, vertical excitation, and nonexcited cases; $L_{nd} = 50.0$ and $\sigma^2_{T,nd} = 1.0$.

a linear mean square response–airspeed relationship, for a much longer airspeed range than the heave response. Indeed, the radial variable of this normal form[6,29] expressed in polar coordinates, $\dot{r} = ar + a_3 r^3$, is essentially characterized by two terms, a linear and a cubic term. Consequently, at steady state, that is, $\dot{r} = 0$, the radial variable increases linearly with the square root of the control parameter $a(U_m)$, or similarly its mean square is a linear function of the control parameter, that is, $r^2 = -a/a_3$, where a is positive and a function of U_m and a_3 is negative for the supercritical Hopf bifurcation. The excited cases follow the same trend.

The other region of interest is the low-speed range. It is at airspeeds well below the flutter point that the presence of longitudinal excitation has the most effect. In some ways, this observation is counterintuitive, when it is considered that, for the pure longitudinal excitation case reported in Ref. 1, the longitudinal excitation evidently exerted no influence at all on the system response below the stochastic flutter point. It appears that, by itself, longitudinal excitation does not have enough energy to excite the system, but may act as a pumping mechanism to amplify the response otherwise created by the vertical component. This behavior is perhaps tied to a phenomenon known in physics as parametric amplification,[2] and it requires further investigation.

Moreover, for a high-turbulence intensity, the response for the combined excitation increases parabolically in this low-airspeed range as airspeed decreases. The probable cause is the lack of structural damping that becomes more evident at low speeds. As the airspeed decreases past $U_{m,nd} \cong 2.5$ (Fig. 6), the aerodynamic damping decreases as well and tends to zero; hence, the airfoil becomes much more sensitive to perturbations. This is true for both the vertically and combined excited cases. For the latter, however, one may interpret the Lyapunov exponent as a mean damping because the aerodynamic damping terms fluctuate according to a Gaussian probability density due to the longitudinal excitation. In this sense, it is conceivable that temporarily (locally in time) the damping becomes zero or negative as the ratio U_m/σ_T goes to zero. In reality, structural damping would be present, and the response would not increase at such a rate. This was confirmed by introducing a small amount of pitch structural damping. The pitch mean square response did not exhibit a parabolic increase, but stabilized on a more realistic value.

A word of caution is offered here: For a combination of very low airspeeds and high-turbulence intensities, the aerodynamic model starts to lose relevance because of possible flow reversal or separation, as well as the turbulence model, which breaks down due to the limitations imposed by Taylor's hypothesis.

The parabolic behavior, or dip, for the combined excitation at low airspeed is also encountered for the linear system; hence, it cannot

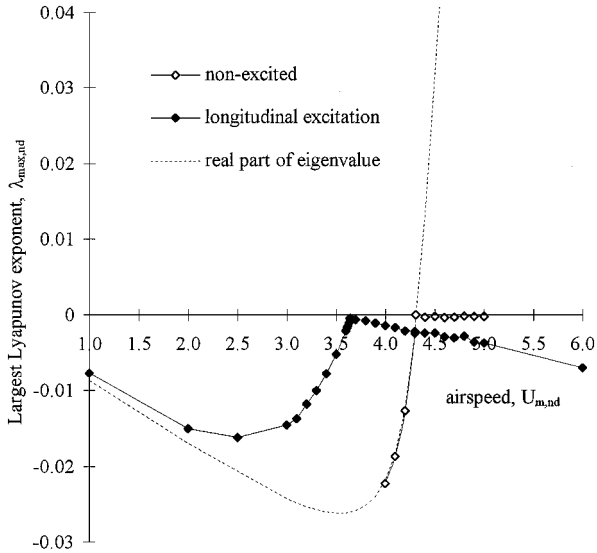

Fig. 6 Largest Lyapunov exponent for the longitudinal excitation and nonexcited cases; $L_{nd} = 50.0$ and $\sigma^2_{T,nd} = 1.0$.

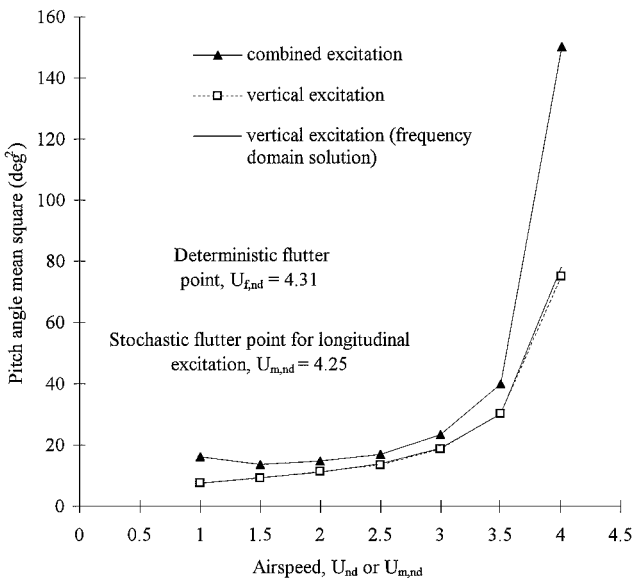

Fig. 7 Linear airfoil pitch mean square response for the combined and vertical excitation cases; $L_{nd} = 0.5$ and $\sigma^2_{T,nd} = 1.0$.

be attributed to the nonlinearity (Fig. 7). Note that, in addition to the numerical solution, the frequency-domain solution for the vertical excitation is shown, the purpose of which is to validate the Runge–Kutta solution. Still, for the linear system, the rate at which the mean square response increases just before the flutter point is higher for the combined excitation than for purely vertical excitation. This is consistent with the advancement of the flutter point due to longitudinal atmospheric turbulence. However, for the nonlinear system in the middle-airspeed range, as the speed is increased through the flutter region no differences in response trends are noted between the combined and vertical excitation cases.

Frequency Content Analysis

The frequency content of the turbulent excited nonlinear airfoil response is first examined in comparison to the linear response. A comparison of the pitch response PSDs (normalized with their respective mean square) is shown in Fig. 8 at a preflutter airspeed. The interplay between the airfoil nonlinearity and turbulence reveals interesting behavior. First, we observe the appearance of a broadband peak not present for the linear problem. It is attributed to an effective stiffness, which is a direct consequence of the torsional stiffness cubic nonlinearity. It is also conjectured that the location of this peak is directly related to the mean square of the response, and moreover,

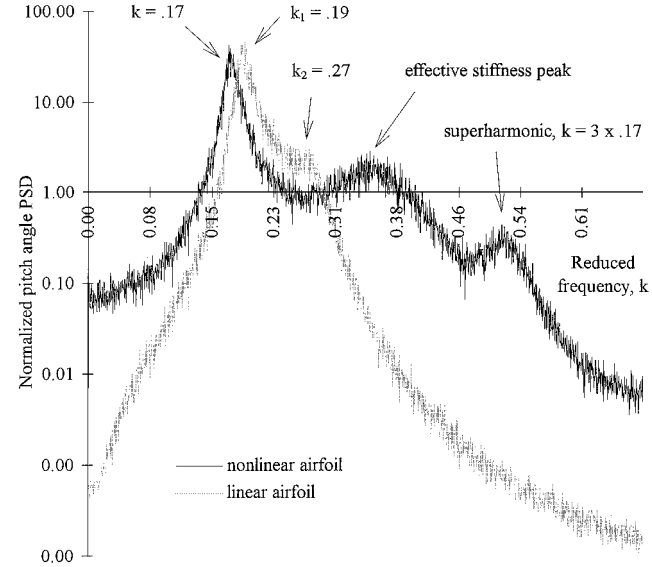

Fig. 8 PSD (normalized by their respective mean square response) of the nonlinear and linear airfoil pitch response for the combined excitation case; $L_{nd} = 50.0$, $\sigma^2_{T,nd} = 0.1$, and $U_{m,nd} = 3.8$.

the relation is proportional. In other words, the greater the response is, the larger the effective stiffness, leading to a higher-frequency band. This point will be made more evident when the combined and vertical excitation cases are compared.

In addition, for the nonlinear airfoil, there is a sharper dominant peak and a lower intensity superharmonic at three times its frequency. For airspeeds above the flutter point, these two peaks define the frequency content of the stochastic LCO and are recovered in the nonexcited, deterministic, problem. For airspeeds below flutter, which is the case shown in Fig. 8, the dominant peak corresponds to the slow linear normal mode, mode 1. It is, however, remarkable that the dominant peak is shifted toward smaller frequencies due to the presence of the nonlinearity. For the case shown in Fig. 8, the frequency of the first linear mode is $k_1 = 0.19$ (note that an eigenvalue analysis gives $k_1 = 0.187$), whereas the frequency of the nonlinear mode is $k = 0.17$. Not shown here, lowering the turbulence excitation level decreases the shift of the nonlinear mode.

The second normal mode, mode 2, involved in the flutter frequency coalescence is not observed in the nonlinear response for the case shown in Fig. 8. We have found that it is only at very low turbulence levels, where nonlinear effects are not important, that this mode starts to appear in the PSD. Finally, no fundamental changes are noticed in the spectra as the airspeed is increased through the flutter point. The lack of distinction of a stochastic Hopf bifurcation in the power spectrum has been observed by Fronzoni et al.[30]

In reference to the second objective of this work, concerning the specific effect of the longitudinal turbulence component, the power spectra for both the combined and vertical excitation cases are essentially the same (Fig. 9). The only difference is a shift of the broadband peak, associated with the effective stiffness, toward a lower frequency for the pure vertical excitation. However, this shift is only evident at lower airspeeds, where there is a large difference in mean square response between the two excitation cases. Note that the presence of the longitudinal component does not appear to change the frequency of the dominant peak.

For the linear problem under combined excitation, some test runs were also conducted to investigate a possible advancement of the frequency coalescence in the vicinity of the flutter point. However, due to the very low damping of the slow mode in this region (hence, extreme sensitivity to the perturbations) and the frequency coalescence itself, which does not permit a clear distinction between modes, it was not possible to deduce any coherent interpretation from the frequency spectrum. Related to the frequency coalescence is the question concerned with the nature of the shift being stiffness or damping related. To investigate this issue, the random excitation quasi steady and apparent mass terms, that is, due to longitudinal turbulence, in the aerodynamic stiffness matrix, and subsequently in the damping

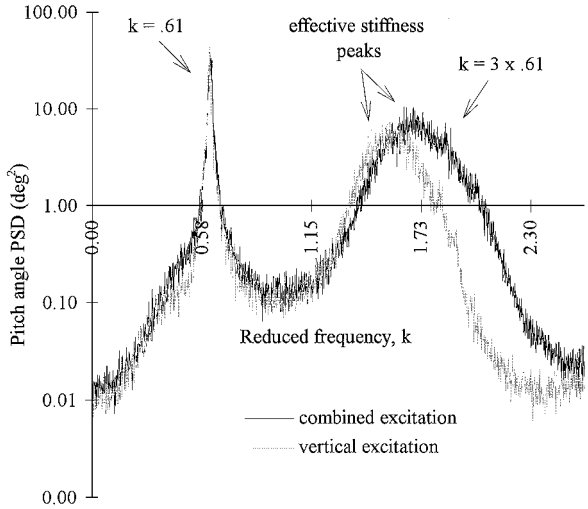

Fig. 9 PSD of the airfoil pitch response for the combined and vertical excitation cases; $L_{nd} = 0.5$, $\sigma^2_{T,nd} = 1.0$, and $U_{m,nd} = 1.0$.

matrix, were artificially neutralized. It was found that the random damping terms had minimal influence, whereas the random stiffness terms essentially dictated the advancement of the flutter point. For example, disabling the random stiffness terms decreased the shift in flutter point from $U_{m,nd} = 3.65$ to 4.27 (compared with 4.31 for the deterministic case), whereas removal of the random damping had essentially no influence. The same observation has been noted by Ibrahim and Heo,[31] but for the response problem.

Lyapunov Exponent Analysis

The Lyapunov exponents express the stability characteristics of a reference trajectory and, more specifically, its sensitivity to small perturbations in initial conditions. They are a generalization of the real part of the eigenvalues, defined for a fixed point, to any arbitrary solution. Given a d-dimensional continuous ergodic system, there exist d nonrandom exponents, some of which could coincide.[4,29] Similarly to the eigenvalue problem, it is the value of the largest exponent, given as λ_{max}, which determines the stability of the trajectory, such that a negative λ_{max} implies a convergence of initially close trajectories whereas a positive λ_{max} defines diverging trajectories. Another characteristic of the Lyapunov exponents is the invariance of their respective magnitude for (almost) any reference trajectory within a given attractor.

No assumption has been made so far on the determinism, or inversely randomness, of the dynamic system. In fact, the concept of Lyapunov exponents has been defined within the framework of random dynamic systems, where the deterministic problem is considered as a particular case of the more general random problem. Examining the d-dimensional linear dynamic system, $\dot{x} = A(t)x$, where A is a randomly time-varying $d \times d$ matrix, it has been shown analytically that a qualitative change in stability, hence, bifurcation, of the random fixed point occurs when the largest Lyapunov exponent changes sign.[4] This change of sign of λ_{max} is also associated with the probabilistic concept of sample stability, also known as stability with probability 1 or almost sure stability. Loosely speaking, sample stability ensures that every sample realization of the system is stable.

Another interpretation of the largest Lyapunov exponent refers to its magnitude, which defines the timescale with which two initially close trajectories converge or diverge with respect to each other. Relatively speaking, a large, but negative, largest Lyapunov exponent is associated with the fast convergence of a strongly stable attractor. As the magnitude of λ_{max} decreases toward zero with a change of control parameter, critical slow down is experienced up to the bifurcation point where λ_{max} vanishes.

A means to obtain the largest Lyapunov exponent is by means of the so-called tangent space method.[32] Although this approach has been applied to calculate the Lyapunov exponents from time series, it is particularly well suited for the case where the equations of motion are available. There are essentially two avenues. One is to linearize the system directly by calculating the Jacobian about the reference, random trajectory $x_r(t)$, hence the requirement to simultaneously integrate numerically the linearized and nonlinear sets of equation. The largest Lyapunov exponent, in nondimensional form, is then obtained with

$$\lambda_{max,nd} = \lim_{\tau \to \infty} \frac{1}{\tau} \ell n \left(\frac{\|\tilde{x}(\tau)\|}{\|\tilde{x}_0\|} \right) \tag{9}$$

where $\tilde{x}$ is the solution of

$$\tilde{x}' = \frac{\partial f(x,\tau)}{\partial x}\Big|_{x_r(\tau)} \tilde{x} = \left[A(\tau) + 3A_3 x^2 \right]\Big|_{x_r(\tau)} \tilde{x} \tag{10}$$

and $f(x,\tau)$ is given by

$$\{x'\} = [A(\tau)]\{x\} + [A_3]\{x^3\} + \{B(\tau)\} = \{f(x,\tau)\} \tag{11}$$

For our problem, $\{x\} = \{\theta, \xi, \theta', \xi', z_1, z_1', z_2, z_2'\}^T$, $[A]$ contains the longitudinal excitation, and $\{B\}$ represents the vertical component of the turbulent excitation. $[A_3]$ is the cubic structural stiffness matrix. Equation (11) is the state-space form of Eq. (8).

The second avenue consists of twice solving the same system of nonlinear equations, with different but close initial conditions, but with the same noise realization. According to Osedelec (see Ref. 4), both approaches should give the same value for λ_{max} because it converges to a finite deterministic value and is invariant for a given attractor.

In this paper we compute the largest Lyapunov exponent with the linearized, variational equations. The second avenue, which involves calculating the Euclidian norm between two neighbor trajectories, excited with the same sample noise, was also performed to obtain some insurance on the validity of the numerical integration. The results shown have also been checked for convergence toward a finite deterministic value as $\tau \to \infty$, as well as invariance from initial conditions and sample noise realization.

Results presented in Fig. 6 are for the longitudinal excitation ($L_{nd} = 50.0$ and $\sigma^2_{T,nd} = 1.0$) and nonexcited nonlinear cases. Also plotted for comparison purposes are the real part of the eigenvalues of the nonexcited linearized system obtained from a standard eigenvalue subroutine. The exponents and eigenvalues shown have been renormalized to a new nondimensional time, $\bar{\tau} = \sigma_T t/b$, vs $U_m t/b$, to get rid of the artificial direct dependence on airspeed.

The following points are noted. The exponents and eigenvalue tend to zero as the airspeed goes to zero. This is a direct consequence of neglecting structural damping. The damping is solely provided by the aerodynamics. Furthermore, the advanced flutter airspeed, due to longitudinal turbulence, at $U_{m,nd} = 3.65$ indicated by the discontinuity in $\lambda_{max,nd}$ confirms the D-bifurcation shown in the PDF diagram of Ref. 1. For the P-bifurcation, which occurs at $U_{m,nd} = 4.71$, no such discontinuity in the largest Lyapunov exponent is noticed.

If we consider the interpretation that the magnitude of the largest Lyapunov exponent is an expression of the degree of stability of trajectories, we may say that longitudinal excitation decreases the stability of the system, strictly speaking the fixed point, on two accounts. Not only does it advance the flutter point, it also decreases the damping or the strength of the attraction; for example, at $U_{m,nd} = 3.0$, $\lambda_{max,nd}$ for the longitudinal excitation is smaller than without noise, thus indicating a longer time to reach steady state. On the flip side, the loss of damping associated with the approach of the flutter speed is more gradual and less explosive with longitudinal turbulence than without. Although the linearized longitudinally excited system is not shown, note that it exhibits the same $\lambda_{max,nd}$ as the nonlinear longitudinally excited airfoil, up to the flutter speed.

Conclusions

In light of the two stated objectives for this paper, and based on the PDF, mean square, frequency, and Lyapunov exponent analysis, the following conclusions are offered.

1) The additional type of dynamic behavior observed for the longitudinal excitation,[1] which separated the stochastic flutter point and LCO onset, does not appear when the vertical component of

turbulence is also considered. Hence, in the combined excitation problem, only two different dynamic regions are observed, characterized by uni- and bimodal PDFs. This is reminiscent of the nonexcited deterministic case, in the sense that the equilibrium point bifurcates directly into a periodic attractor, without first transitioning through an additional attractor whose nature is purely due to the interplay of the nonlinearity and parametric random excitation. Thus, we are tempted to extend the concept of bifurcation robustness and structural stability applied to deterministic systems[29] and to propose that, because both longitudinal and vertical random excitations are present in reality, the bifurcation scenario observed for pure longitudinal excitation is qualitatively not robust.

2) The advancement of the flutter point observed for pure longitudinal excitation[1] is also present when the vertical component is added. This is shown to be the case for both the linearized and nonlinear problems, although for the latter case, the flutter point coincides with the supercritical Hopf bifurcation in the form of a P-bifurcation.

3) The presence of longitudinal excitation decreases the stability of the system, strictly speaking the fixed point, in preflutter conditions on two accounts. Not only does it advance the flutter point, but it also diminishes the damping for airspeed below flutter as shown by the Lyapunov exponents.

4) The frequency spectra do not seem to indicate an influence of longitudinal turbulence on the system modal frequencies, hence an eventual shift in the frequency coalescence associated with flutter. However, a parametric analysis demonstrates that the advancement of the flutter point is determined essentially by the random aerodynamic stiffness, not by the damping terms. The nature of the shift of the flutter point is, thus, stiffness related, typical of the deterministic classical flutter problem.

5) The interplay between the airfoil nonlinearity and turbulent excitation has the following effects on the response PSD. In comparison with the linear problem, the dominant peak in the nonlinear response, which is associated with the lightly damped linear mode, is shifted toward smaller frequencies. In addition, a lower intensity peak appears at three times the frequency of the dominant peak, as well as a broadband peak, which we have interpreted as being related to an effective stiffness.

6) From a more phenomenological perspective, it is observed that turbulence may advance the airspeed at which the pitch angle marginal PDF changes from a uni- to bimodal when compared with the nonexcited deterministic case, whereas the heave transition appears to be postponed. This observation is attributed to the location of the nonlinearity, which is positioned at the elastic axis and acting on the torsional spring.

7) Finally, the impact of the longitudinal excitation on the otherwise vertically excited mean square pitch and heave responses is generally more important at low rather than high airspeeds. At low speeds, the randomly varying aerodynamic damping exhibits temporary zero or negative values, such that the airfoil becomes very sensitive to perturbations, namely, vertical turbulence. At higher speed, the difference in the nonlinear mean square responses between pure vertical excitation and the combined excitation tends to settle on a constant value, for both pitch and heave.

Acknowledgments

The authors gratefully acknowledge the support of the Department of National Defence and the Natural Sciences and Engineering Research Council of Canada.

References

[1]Poirel, D. C., and Price, S. J., "Post-Instability Behavior of a Structurally Nonlinear Airfoil in Longitudinal Turbulence," *Journal of Aircraft*, Vol. 34, No. 5, 1997, pp. 619–626.

[2]Stratonovich, R. L., *Topics in the Theory of Random Noise; Peaks of Random Functions and the Effect of Noise on Relays and Nonlinear Self-Excited Oscillations in the Presence of Noise*, Vol. 2, Gordon and Breach, New York, 1967.

[3]Ibrahim, R. A., *Parametric Random Vibrations*, Research Studies Press, Wiley, New York, 1985.

[4]Arnold, L., Jones, C., Mischaikow, K., and Raugel, G., *Dynamical Systems*, Springer-Verlag, Berlin, 1995.

[5]Horsthemke, W., and Lefever, R., *Noise-Induced Transitions; Theory and Applications in Physics, Chemistry and Biology*, Springer-Verlag, Berlin, 1984.

[6]Knobloch, E., and Weisenfeld, K. A., "Bifurcations in Fluctuating Systems: The Center Manifold Theory," *Journal of Statistical Physics*, Vol. 33, No. 3, 1983, pp. 611–637.

[7]Ariaratnam, S. T., "Some Illustrative Examples of Stochastic Bifurcation," *Nonlinearity and Chaos in Engineering Dynamics*, edited by J. M. T. Thompson and S. R. Bishop, Wiley, New York, 1994, pp. 267–274.

[8]Lee, B. H. K., Brown, D., Zgela, M., and Poirel, D., "Wind Tunnel Investigation and Flight Tests of Tail Buffet on the CF-18 Aircraft," CP-483, AGARD, 1990, pp. 1–26.

[9]Ibrahim, R. A., Orono, P. O., and Madaboosi, S. R., "Stochastic Flutter of a Panel Subjected to Random In-Plane Forces, Part 1: Two Mode Interaction," *AIAA Journal*, Vol. 28, No. 4, 1990, pp. 694–702.

[10]Abdel-Motagaly, K., Duan, B., and Mei, C., "Nonlinear Panel Response at High Acoustic Excitations and Supersonic Speeds," *Proceedings of the 40th Structures, Structural Dynamics, and Materials Conference*, AIAA, Reston, VA, 1999, pp. 1518–1529.

[11]Romberg, O., and Popp, K., "The Influence of Upstream Turbulence on the Stability Boundaries of a Flexible Tube in a Bundle," *Journal of Fluids and Structures*, Vol. 12, No. 2, 1998, pp. 153–169.

[12]Le Maître, O., Huberson, S., and Souza De Cursi, E., "Unsteady Model of Sail and Flow Interaction," *Journal of Fluids and Structures*, Vol. 13, No. 1, 1999, pp. 37–59.

[13]Lin, Y. K., "Stochastic Stability of Wind-Excited Long-Span Bridges," *Probabilistic Engineering Mechanics*, Vol. 11, No. 4, 1996, pp. 257–261.

[14]Prussing, J. E., and Lin, Y. K., "Rotor Blade Flap-Lag Stability in Turbulent Flows," *Journal of the American Helicopter Society*, Vol. 27, April 1982, pp. 51–57.

[15]"Military Specification, Airplane Strength and Rigidity Flight Loads," MIL-SPEC Mil-A-8861B(AS), Amendment 1, 5 Dec. 1994.

[16]"Military Specification, Airplane Strength and Rigidity Vibration, Flutter and Divergence," MIL-SPEC Mil-A-8870C(AS), 25 March 1993.

[17]Hoblit, F. M., *Gust Loads on Aircraft: Concepts and Applications*, AIAA Education Series, AIAA, New York, 1988, pp. 1–51.

[18]Houbolt, J. C., Steiner, R., and Pratt, K. G., "Dynamic Response of Airplanes to Atmospheric Turbulence Including Flight Data on Input and Response," NASA TR R-199, 1964.

[19]Fung, Y. C., *An Introduction to the Theory of Aeroelasticity*, Wiley, New York, 1955, pp. 206–212, 294–298.

[20]Lin, C. C., *Statistical Theories of Turbulence*, Princeton Univ. Press, Princeton, NJ, 1961, pp. 9–12.

[21]Van der Wall, B. G., and Leishman, J. G., "On the Influence of Time-Varying Flow Velocity on Unsteady Aerodynamics," *Journal of the American Helicopter Society*, Vol. 39, No. 4, 1994, pp. 25–36.

[22]Leishman, J. G., "Unsteady Lift of a Flapped Airfoil by Indicial Concepts," *Journal of Aircraft*, Vol. 31, No. 2, 1994, pp. 288–297.

[23]Press, W. H., Teukolsky, S. A., Vetterling, W. T., and Flannery, B. P., *Numerical Recipes in Fortran: The Art of Scientific Computing*, Cambridge Univ. Press, Cambridge, England, U.K., 1996, pp. 195–199.

[24]Fujimori, Y., Lin, Y. K., and Ariaratnam, S. T., "Rotor Blade Stability in Turbulent Flows, Part 2," *AIAA Journal*, Vol. 17, No. 7, 1979, pp. 673–678.

[25]Lee, B. H. K., Brown, D., Tang, F. C., and Plosenki, M., "Flowfield in the Vicinity on an F/A-18 Vertical Fin at High Angles of Attack," *Journal of Aircraft*, Vol. 30, No. 1, 1993, pp. 69–74.

[26]Mackey, M. C., Longtin, A., and Lasota, A., "Noise-Induced Global Asymptotic Stability," *Journal of Statistical Physics*, Vol. 60, Nos. 5/6, 1990, pp. 735–751.

[27]Lugiato, L. A., Broggi, G., Merri, M., and Pernigo, M. A., "Control of Noise by Noise and Applications to Optical Systems," *Noise in Nonlinear Dynamical Systems*, Cambridge Univ. Press, Cambridge, England, U.K., Vol. 2, 1989, pp. 293–346.

[28]Schimansky-Geier, L., Tolstopjatenko, A. V., and Ebeling, W., "Noise Induced Transitions Due to External Additive Noise," *Physics Letters*, Vol. 108A, No. 7, 1985, pp. 329–332.

[29]Argyris, J., Faust, G., and Haase, M., *An Exploration of Chaos; An Introduction for Natural Scientists and Engineers*, North-Holland, Amsterdam, 1994, pp. 173–180, 308–320.

[30]Fronzoni, L., Mannella, R., McClintock, P. V. E., and Moss, F., "Postponement of Hopf Bifurcations by Multiplicative Colored Noise," *Physical Review A: General Physics*, Vol. 36, No. 2, 1987, pp. 834–841.

[31]Ibrahim, R. A., and Heo, H., "Stochastic Response of Nonlinear Structures with Parameter Random Fluctuations," *AIAA Journal*, Vol. 25, No. 2, 1987, pp. 331–338.

[32]Schreiber, T., "Interdisciplinary Application of Nonlinear Time Series Methods," *Physics Report*, Vol. 308, No. 1, 1999, pp. 1–64.

A. M. Baz
Associate Editor